HMG Advance Access published September 2, 2010

Human Molecular Genetics, 2010 **1–10**
doi:10.1093/hmg/ddq341

Molecular signature of primary retinal pigment epithelium and stem-cell-derived RPE cells

Jo-Ling Liao[1], Juehua Yu[1], Kevin Huang[1], Jane Hu[2], Tanja Diemer[2], Zhicheng Ma[1], Tamar Dvash[1], Xian-Jie Yang[2], Gabriel H. Travis[2], David S. Williams[2], Dean Bok[2] and Guoping Fan[1,*]

[1]Department of Human Genetics and [2]Jules Stein Eye Institute, David Geffen School of Medicine, University of California Los Angeles, Los Angeles, CA, USA

Received May 26, 2010; Revised July 25, 2010; Accepted August 9, 2010

Age-related macular degeneration (AMD) is characterized by the loss or dysfunction of retinal pigment epithelium (RPE) and is the most common cause of vision loss among the elderly. Stem-cell-based strategies, using human embryonic stem cells (hESCs) or human-induced pluripotent stem cells (hiPSCs), may provide an abundant donor source for generating RPE cells in cell replacement therapies. Despite a significant amount of research on deriving functional RPE cells from various stem cell sources, it is still unclear whether stem-cell-derived RPE cells fully mimic primary RPE cells. In this report, we demonstrate that functional RPE cells can be derived from multiple lines of hESCs and hiPSCs with varying efficiencies. Stem-cell-derived RPE cells exhibit cobblestone-like morphology, transcripts, proteins and phagocytic function similar to human fetal RPE (fRPE) cells. In addition, we performed global gene expression profiling of stem-cell-derived RPE cells, native and cultured fRPE cells, undifferentiated hESCs and fibroblasts to determine the differentiation state of stem-cell-derived RPE cells. Our data indicate that hESC-derived RPE cells closely resemble human fRPE cells, whereas hiPSC-derived RPE cells are in a unique differentiation state. Furthermore, we identified a set of 87 signature genes that are unique to human fRPE and a majority of these signature genes are shared by stem-cell-derived RPE cells. These results establish a panel of molecular markers for evaluating the fidelity of human pluripotent stem cell to RPE conversion. This study contributes to our understanding of the utility of hESC/hiPSC-derived RPE in AMD therapy.

INTRODUCTION

Age-related macular degeneration (AMD) is a severe retinal disease that significantly impairs vision. In the western world, AMD is the leading cause of blindness among the elderly, affecting over 30 million people worldwide (1). AMD patients are usually afflicted with degenerated and/or dysfunctional retinal pigment epithelium (RPE), which normally plays various central roles in maintaining retinal integrity and viability (2). In particular, RPE is involved in the formation of the blood-retinal barrier, absorption of stray light, supplying of nutrients to the neural retina, regeneration of visual pigment, as well as the uptake and recycling of the outer segments of photoreceptors. Consequently, loss of RPE leads to photoreceptor depletion and irreversible blindness (3). Current treatments for AMD are severely limited. Palliative treatment options are only available for the less prevalent, 'wet' form of the disease, including the use of anti-neovascular agents, photodynamic therapy and thermal laser therapy. However, there are no current treatments for the more widespread, 'dry' AMD except for the use of antioxidants to delay disease progression in the eye. Despite current treatments, patients with 'dry' AMD generally show poor prognosis and eventual loss of vision (4).

Cell therapy holds tremendous promise in treating AMD; directly replenishing the degenerated RPE can restore retinal function and rescue vision in AMD patients. Autologous RPE/choroid transplant attempts from periphery to central retina have demonstrated partial restoration of vision in AMD patients (5). However, autologous transplantation is limited by the scarcity and genetic predisposition to AMD of the cell source, which may affect the efficacy of transplantation (5). Pluripotent stem cells have been proposed to be

*To whom correspondence should be addressed at: Department of Human Genetics, David Geffen School of Medicine, UCLA, 695 Charles Young Drive South, Los Angeles, CA 90095, USA. Tel: +1 3102670439; Fax: +1 3107945446; Email: gfan@mednet.ucla.edu

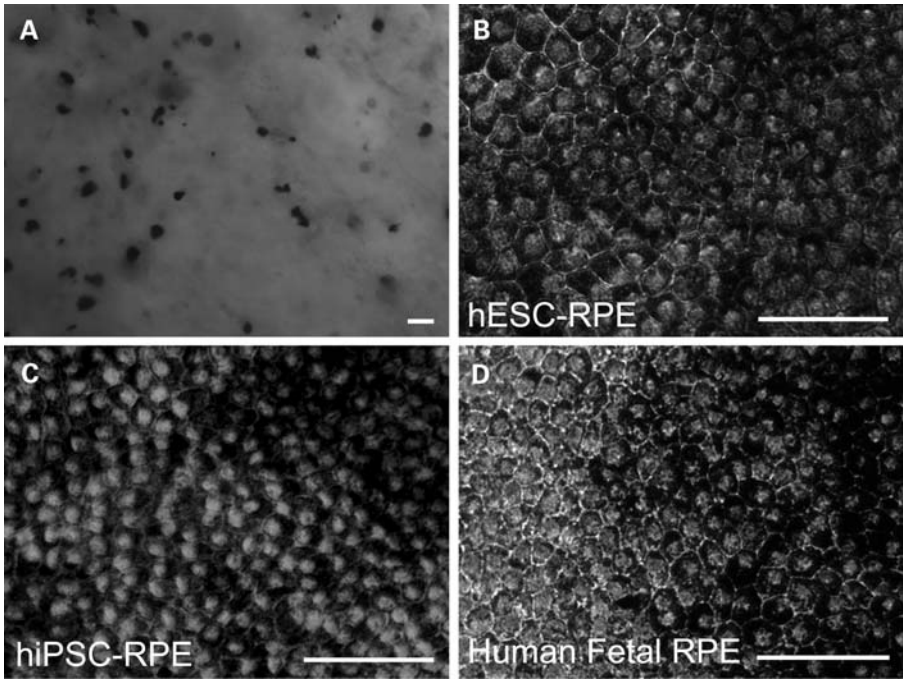

Figure 1. Morphology of fetal-RPE, HESC-RPE and hiPSC-RPE. (**A**) Pigmented cells appear as discrete clusters after 3–4 weeks of hESCs or hiPSCs differentiation. (**B**–**D**) HESC-RPE cells, hiPSC-RPE and human fRPE cells are morphologically very similar under high magnification. Scale bars: (A), 100 μm; (B–D), 50 μm.

an attractive alternative cell source for transplantation. Human embryonic stem cells (hESCs) can indefinitely self-renew and differentiate into any cell type found in the adult body, making hESCs a promising candidate for generating an unlimited donor source for RPE transplantation (6). In addition, recent derivation of human-induced pluripotent stem cells (hiPSCs) by forced expression of four transcription factors (Oct4, Sox2, c-myc, Klf4) in fibroblasts has created an additional cell source for cell therapy (7). Various studies report that hiPSCs closely resemble hESCs and have been proposed to be promising surrogates for hESCs (7–9). HiPSCs have the added advantage of avoiding immunological complications and ethical controversies that are typically associated with handling hESCs (10). In addition, hiPSCs have the potential to become a platform for personalized medicine by allowing a patient's own cells to become a source for therapeutic tissue (11).

Previous studies on differentiating RPE cells from stem cells demonstrate that stem-cell-derived RPE cells have molecular characteristics similar to primary RPE cells (2,12,13). In addition, the transplantation of stem-cell-derived RPE can partially restore visual function in the retinal dystrophy rat model (12,14,15). However, despite a significant amount of research on the derivation of functional RPE cells from various stem cell sources, no systemic comparison has been done between these stem-cell-derived RPE cells and primary RPE cells. In order to realize the therapeutic potential of stem-cell-derived RPE cells, it is important to ensure that stem-cell-derived RPE cells can recapitulate both functional and genetic characteristics of primary RPE cells.

RESULTS

Differentiation and expansion of putative RPE cells from hESCs and hiPSCs

To determine the ability of various lines of hESCs and hiPSCs to differentiate into RPE cells, we followed a previously described differentiation protocol using a total of 11 cell lines (Supplementary Material, Table S1) (12). Pigmented cells spontaneously arise from differentiating hESCs and hiPSCs after 3–4 weeks of culture in bFGF-free hESC culture media. Pigmented clusters grew in size and number after an additional 2–3 weeks of culture. Although all cell lines were able to generate pigmented clusters reproducibly, various lines of hESCs and hiPSCs displayed varying differentiation efficiencies. H9 and H1 lines showed the highest efficiencies, giving rise to over 200 pigmented clusters per cell culture dish (Fig. 1A). HUES12, HUES15 and HSF1 cell lines showed fairly similar efficiencies with about 150 pigmented clusters. HSF6 cell lines showed relatively lower efficiencies giving rise to less than 100 pigmented clusters. All lines of hiPSCs gave rise to approximately 150 pigmented clusters, despite different parental cell types. HiPS cell lines derived from neuroectoderm and endoderm lineage both generated pigmented clusters at similar efficiencies.

Stem-cell-derived pigmented clusters were manually excised and expanded to monolayers on Matrigel. These stem-cell-derived pigmented sheets appeared homogenous in the inner part of a cluster; however, cells on the edges generally showed less pigment, suggesting that they may be in a less differentiated state. This observation is consistent with previous reports that stem-cell-derived RPE cells expand by

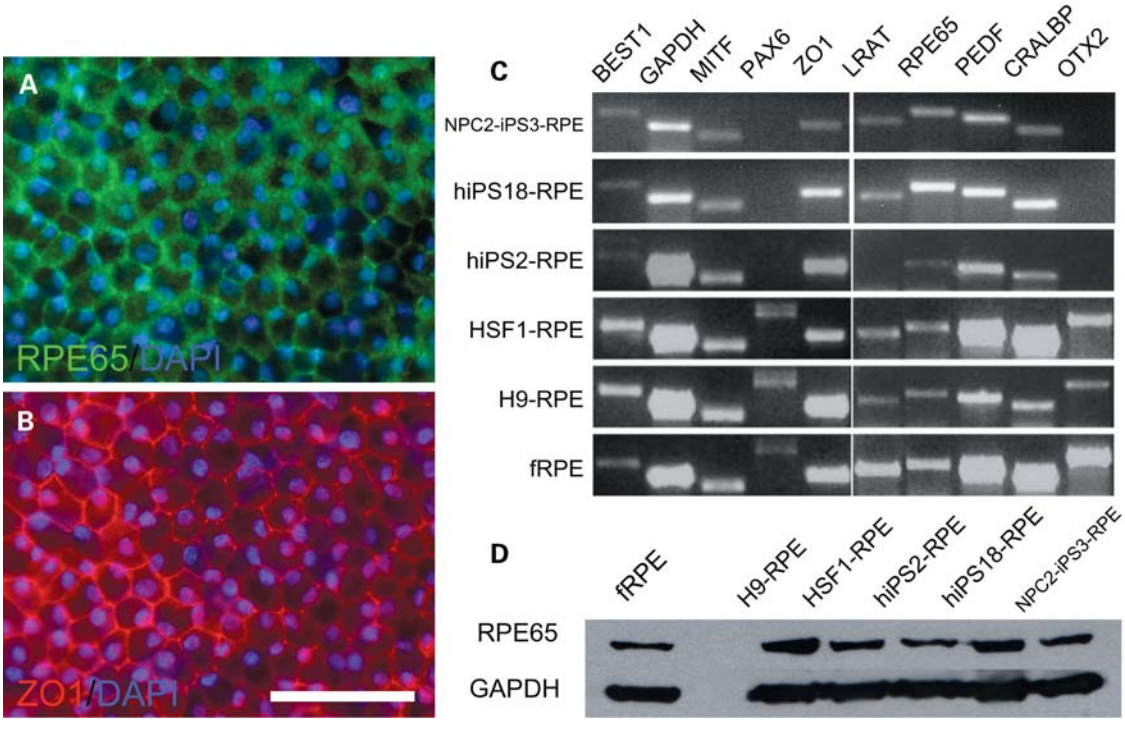

Figure 2. Stem-cell-derived RPE exhibit characteristic marker genes of fRPE. (**A**) and (**B**) are immunoluorescent labeling of RPE65 and ZO1 in hESC-RPE, respectively. (**C**) RT–PCR analysis of human fRPE gene markers in different lines of hESC-RPE and hiPSC-RPE. (**D**) Western blot analysis of RPE65 and GAPDH proteins in hESC-RPE, hiPSC-RPE and fRPE. Human fRPE cells cultured for 3 months *in vitro* were used as a positive control in this assay. Scale bar: (A) and (B), 50 μm.

de-differentiation, proliferation and then re-differentiate to acquire pigmentation (12). The stem-cell-derived pigmented sheets were cultured for 2–3 months and characterized through various molecular and functional assays. We pursued and characterized the lines that could be most efficiently differentiated (H9-RPE, HSF1-RPE, HiPS2-RPE, HiPS18-RPE and NPC2-iPS#3-RPE). HESC-RPE and hiPSC-RPE expanded sheets exhibited polygonal, cobblestone-like morphology under bright field microscopy, consistent with normal fetal RPE (fRPE) cell morphology (Fig. 1). Electron micrograph results revealed that hESC-RPE have apical microvilli, basal end-feet and melanin structures similar to human RPE (Supplementary Material, Fig. S1A). We observed a small number of flattened cells scattered beneath the hESC-RPE monolayer. These non-RPE cells resemble fibroblasts and are embedded in Matrigel substrate. Overall, consistent with previous reports, our results indicate that multiple lines of hESCs and hiPSCs can spontaneously differentiate to clustered pigmented cells, which further differentiate into monolayer RPE-like cells in defined culture environments.

Stem-cell-derived RPE cells express genes and proteins associated with primary RPE cells

To further determine whether hESC-RPE and hiPSC-RPE mimic normal RPE cells, we asked if these stem-cell-derived RPE cells express the appropriate RPE markers. Using reverse transcription–polymerase chain reaction (RT–PCR), we assayed for the expression of several known genes that are expressed in human fRPE cells. We first examined the regulatory gene transcripts central to RPE development, including the early eye field development marker, PAX6 and RPE-specific transcription factors MITF and OTX2. Both MITF and OTX2 are necessary for RPE differentiation; in particular, MITF is known to be associated with the onset and maintenance of pigmentation and is an established marker of RPE during the course of eye development. We also examined the expression of RPE functional markers in stem-cell-derived cells. These markers include the secreted (PEDF), membrane-associated proteins (BEST1, ZO1) and most importantly, the visual cycle proteins (RPE65, LRAT, CRALBP). For comparison, 3 months *in vitro*, cultured human fRPE cells (16) were used as a positive control in all assays.

Interestingly, RT–PCR detected PAX6 in hESC-RPE and fRPE but not in hiPSC-RPE. MITF and OTX2 were both detected in hESC-RPE and fRPE, whereas hiPSC-RPE expressed only MITF but not OTX2. Secreted and membrane-bound protein such as PEDF, BEST1 and ZO1 were seen in all stem-cell-derived RPE cells. Furthermore, RPE65, LRAT and CRALBP transcripts were detected in both types of stem-cell-derived RPEs (Fig. 2C). In addition, RPE65 protein expression was confirmed in both hiPSC-RPE and hESC-RPE by immunoblots (Fig. 2D). These results indicate that both hESC-RPE and hiPSC-RPE exhibit many functional markers characteristic of primary fRPE cells. Moreover, hESC-RPE more closely resembles fRPE than hiPSC-RPE, whereas hiPSC-RPE appears to be in a unique differentiation state.

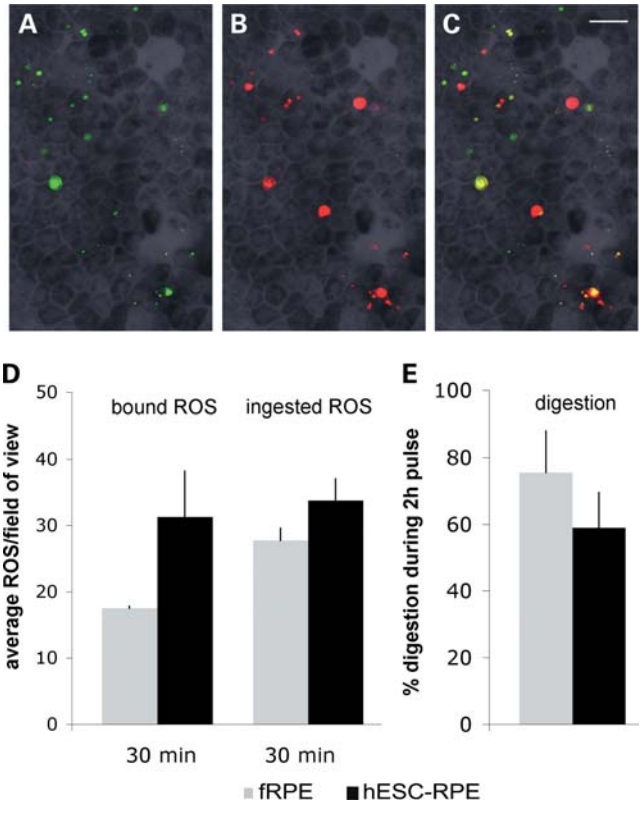

Figure 3. Quantification of phagocytosis of ROSs. (**A**–**C**) Immunofluorescence images of hESC-derived RPE cells after incubation with ROSs. Bound ROSs were labeled with opsin antibody before permeabilization of the cells (green). Bound and ingested ROSs were both labeled with a different colored secondary antibody (red) after permeabilization. Bound ROSs therefore appear green in the upper panel and yellow in the lower panel. Ingested ROSs appear red in the middle and lower panels. Scale bar = 20 μm. (**D**) The number of bound and ingested ROSs after 30 min incubation with the ROSs. (**E**) The digestion of ingested ROSs during the 2 h 'pulse', after the 30 min incubation with ROSs, expressed as the percentage decrease of ingested ROSs during the pulse. Error bars are s.e.m.

To determine whether hESC-RPE has a definitive phagocytic function, we first examined microarray data and found that expression of phagocytic genes (MERTK, LAMP2, VDP and GULP1) are comparable between hESC-RPE and fRPE (see below). Second, using a previously characterized cell culture assay, we compared the ability of the hESC-RPE cells to bind, ingest and digest mouse rod outer segments (ROSs) disk membranes with that of human fRPE cells. After 30 min incubation with isolated ROSs, the hESC-RPE cells had nearly twice as many ROSs bound to their surface, although the number of ingested ROSs was comparable to fRPE cells (Fig. 3). The rate of digestion was determined by comparing the number of ROSs remaining in the cells after subsequent 2 h incubation in the absence of ROSs. The calculated proportion of ROSs digested during this period was similar in the hESC-RPE and fRPE cells (Fig. 3). The hESC-RPE cells therefore appeared comparable to fRPE cells in their ability to ingest and digest ROSs. There was, however, a difference in the number of ROSs that bound to the cell surface. Even after the 2 h incubation in the absence of ROSs, hESC-RPE had many more ROSs bound to their surface (~20 ROSs/field of view), suggesting that they may express more ROS receptor that is not involved with ingestion.

Transcriptome analysis of fRPE, hESC-derived RPE and hiPSC-derived RPE

In order to gain a more comprehensive understanding of the differentiation state of stem-cell-derived cells, we generated global gene expression profiles of stem-cell-derived RPE cells and compared them with native fRPE, primary culture fRPE cells, undifferentiated hESCs and fibroblasts. Probe intensity signals were quantile-normalized and log-transformed across samples using the limma package in Bioconductor. To increase the statistical power of our analysis, we incorporated microarray data sets of various hESCs and somatic tissues including brain, liver, lung and melanocytes from the Gene Expression Omnibus (GEO) database (Supplementary Material, Table S2).

To determine the degree of similarity or difference between stem-cell-derived RPE cells and other cells and tissues, we first performed hierarchical clustering and principal component analysis (PCA). Hierarchical cluster and PCA both demonstrate distinct separation of undifferentiated hESCs, somatic tissues and native/cultured fRPE clusters. As expected, both methods show technical replicates of somatic cells cluster closer together in comparison with clusters of similar biological samples (Fig. 4). The dendrogram shows that hESC-RPE clustered together with fRPE whereas hiPSC-RPE clustered away from the fRPE. Importantly, stem-cell-derived RPE cells do not cluster together with human melanocytes, which is another pigmented cell type derived from neural crest. For PCA analysis, we focussed on the first three principal components, which captured over 70% of the total variance. Consistent with hierarchical clustering results, biplots between the first three principal components revealed close clustering of stem-cell-derived RPE cells and fRPE while clustering away from both hESCs and somatic cells (Fig. 4C and D).

Furthermore, pair-wise comparisons between gene expression profiles show more similarity between hESC-RPE and fRPE than between hiPSC-RPE and fRPE (Fig. 4A). This is further supported by a higher Pearson correlation between hESC-RPE and fRPE cells. In addition, both lines of hESC-RPE are well correlated with each other (Pearson's correlation = 0.948). The comparison of hESC-RPE and fRPE data sets revealed 88 transcripts that were differentially expressed at least 1.5-fold, 39 of which were up-regulated and 49 were down-regulated. Gene ontology revealed that up-regulated genes in hESC-RPE correspond to biological processes such as cell proliferation and neuronal differentiation, whereas down-regulated genes were associated with visual perception and gas transport. The comparison of hiPSC-RPE and fRPE data revealed 224 transcripts that were differentially expressed, 30 of which were up-regulated and 194 were down-regulated. The down-regulated genes in hiPSC-RPE, similar to hESC-RPE, are involved in gas transport and visual perception. Interestingly, an analysis of over-expressed transcripts in hiPSC-RPE revealed that the majority of these genes are involved in epithelial development and the inflammatory response. Notably, gene network analysis of

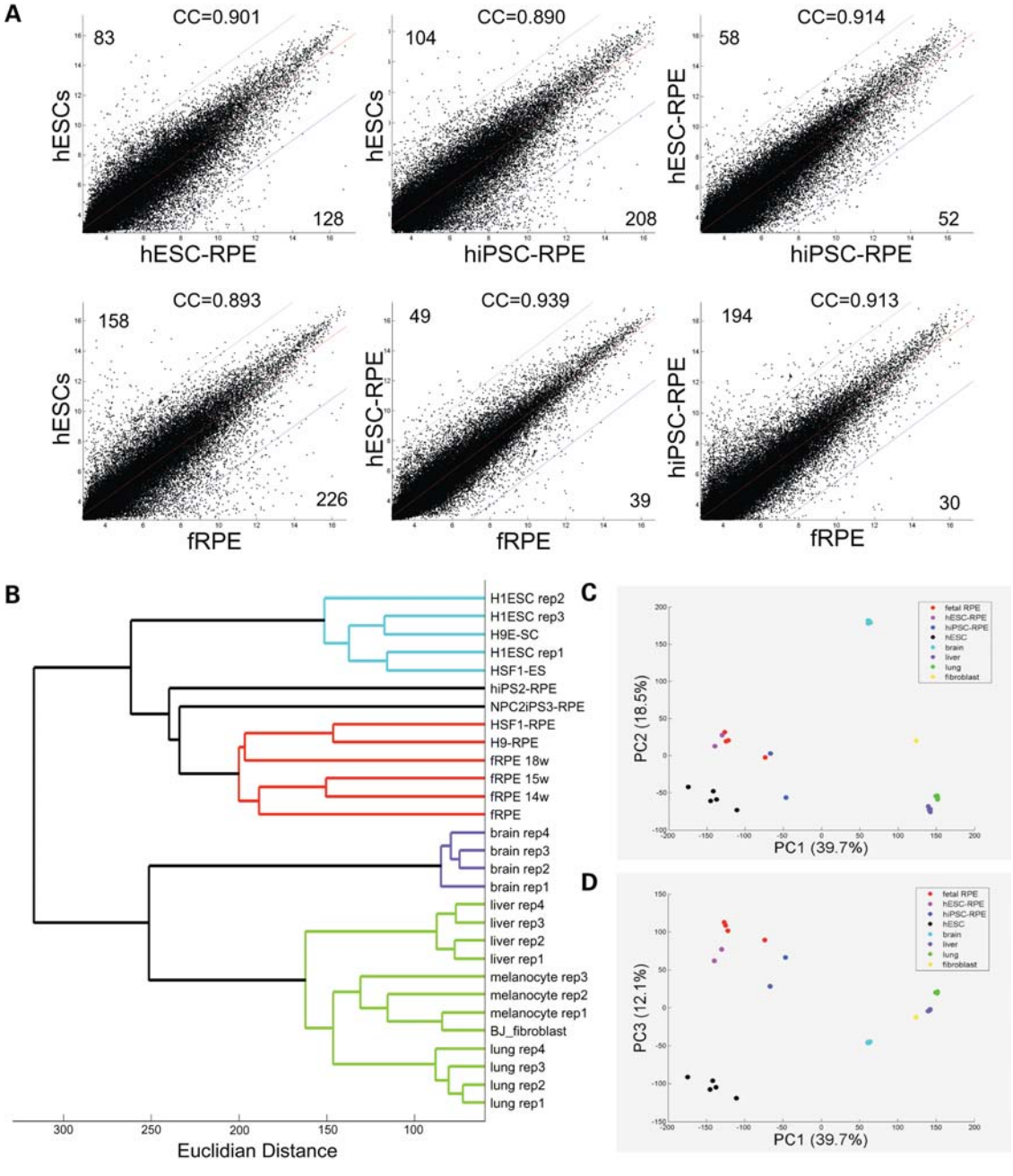

Figure 4. Microarray analysis of genome-wide gene expression of primary fRPE and stem-cell-derived RPE cells. (**A**) Pair-wise comparisons between fRPE, hESCs and stem-cell-derived RPE cells. Linear regression lines are shown in red and the green curves represent $P = 0.05$. Data points outside the green curve represent genes that have significant, differential expression in each cell type. Numbers above the green curve indicate the total number of genes that are up-regulated in the *y*-axis, and numbers below the green curve represent genes up-regulated on the *x*-axis. Pearson's correlation coefficients are shown for comparison of each data set. (**B**) Unbiased hierarchical clustering showing hESC-RPE cluster closer to fRPE than to hiPSC-RPE. Various somatic tissues and additional hESCs from GEO database were included in gene expression analysis to increase statistical power. (**C** and **D**) Biplots of three predominant principal components (PC1, PC2 and PC3) demonstrate that samples cluster to three distinct groups of somatic tissues, hESCs and RPE.

multiple lines of hESCs and hiPSCs also identified many immune response genes that are significantly differentially expressed between hESCs and hiPSCs (unpublished data). This suggests that hiPSC-RPE may retain the gene signatures of hiPSCs. Overall, these data indicate that hESC-RPE is reproducibly more closely related to fRPE than hiPSC-RPE.

Stem-cell-derived RPE cells express low levels of marker genes associated with aging and AMD

We examined genes that are involved in RPE differentiation, pigment synthesis, phagocytic activity and vitamin A metabolism. HESC-RPE showed comparable expression levels with fRPE for the majority of these genes (Fig. 5A). We

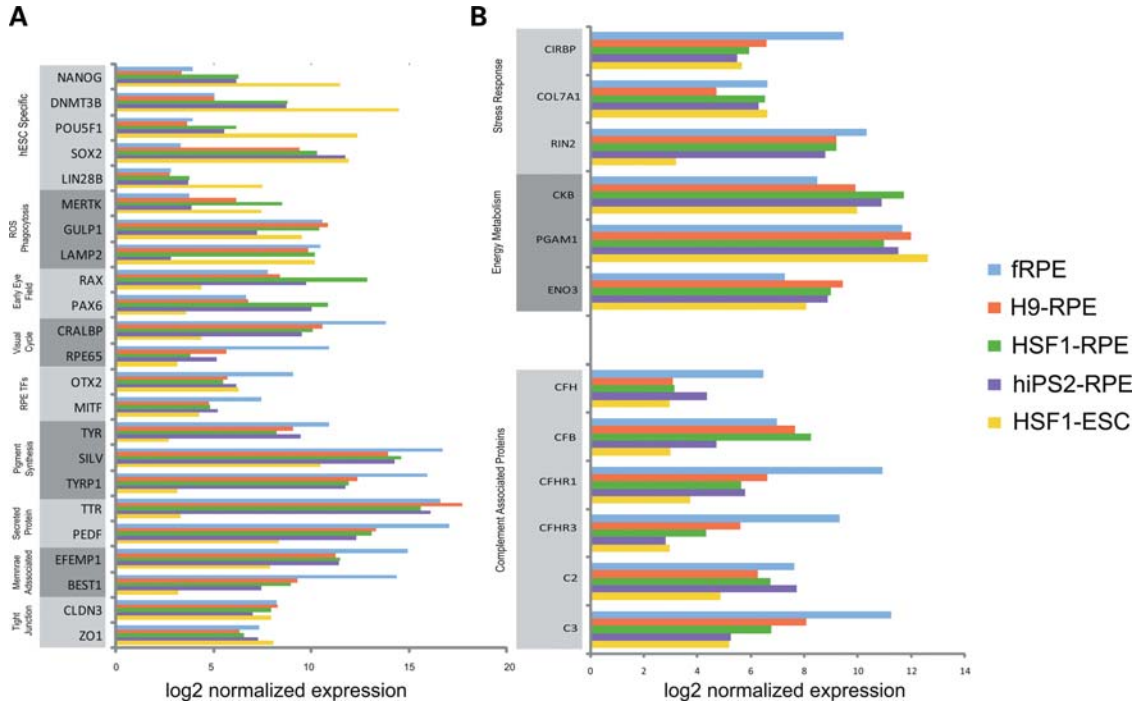

Figure 5. Comparative analysis of gene expression levels for pluripotency and RPE-related genes in hESCs, hESC-RPE, hiPSC-RPE and fRPE. Normalized expression levels were obtained from Agilent whole-genome microarrays. (**A**) Genes that are significantly expressed in pluripotent stem cells and RPE-associated markers were selected. RPE-associated markers are expressed in hESC-RPE, many at levels close to human fRPE cells. Two technical replicates were used for all cell types. (**B**) Expression of genes associated with aging retina and complement cascades.

next examined whether stem-cell-derived RPE cells express genes involved in AMD pathogenesis. AMD is considered a complex genetic disease involving interactions between multiple genes and environmental risk factors, with age and family history being the two strongest risk factors. In addition, recent genetic studies have shown strong association between single nucleotide polymorphism (SNP) variants in complement cascade, components of the innate immune system and AMD pathogenesis (17). We examined the expression of genes which were previously identified to be differentially expressed in young and aging human retina (18), including genes involved in energy metabolism (CKB, PGAM1, ENO3) and stress response (CIRBP, COL7A1, MACS). We observed a low level of expression for both metabolic and stress response genes in stem-cell-derived RPE cells and fRPE. These results indicate that stem-cell-derived RPE cells, though subjected to culture conditions, showed similar energy metabolism and stress response as normal fRPE.

Furthermore, we looked at expression of common genes involved in the complement cascade. A number of complement system protein variants and complement regulatory protein variants are shown to be strongly associated with AMD (17,19). These include complement factor H, complement factor B, complement component 2 (C2) and complement component 3 (C3). Stem-cell-derived RPE showed comparable expression levels to fRPE in all of the complement factor genes we examined (Fig. 5B). Overall, these results indicate that stem-cell-derived RPE cells express a normal level of many RPE-associated markers as well as genes associated with complement regulation.

Human RPE have distinct signature genes from stem-cell-derived RPE cells

A recent comprehensive study comparing gene expression profiles of fetal and adult RPE with somatic tissues identified 154 signature genes that are unique to RPE (20). We asked if these RPE signature genes can be used to classify fRPE, stem-cell-derived RPE and hESCs. Our cross-reference analysis showed that 151 candidate signature genes in their Affymetrix platform can be identified in our Agilent microarray. Among these 151 signature genes, we found that 43 genes were not significant in the differential expression between fRPE and hESCs (Supplementary Material, Table S3). Gene ontology analysis revealed that these genes are associated with protein transport and fatty acid metabolism, suggesting that RPE may share many metabolic properties with hESCs (Fig. 6B). Although these 43 genes are not significantly differentially expressed between hESCs, it does not exclude the possibility that these genes are important for RPE maintenance. Of the remaining 108 RPE signature genes, 87 genes showed robust expression in fRPE, suggesting that these 87 fRPE-specific genes better represent true RPE signature genes (Fig. 6A). Consistent with global gene expression comparison as seen in Fig. 4, hESC-RPE also shared more signature genes with fRPE than hiPSC-RPE. Venn diagram analysis of fRPE, hESC-RPE and hiPSC-PRE indicated 42 genes are commonly shared by these cells, suggesting that these 42 genes are the core RPE differentiation genes (Fig. 6A). Gene ontology analysis indicated that these genes are involved in various pigmentation, visual perception and eye development pathways, consistent

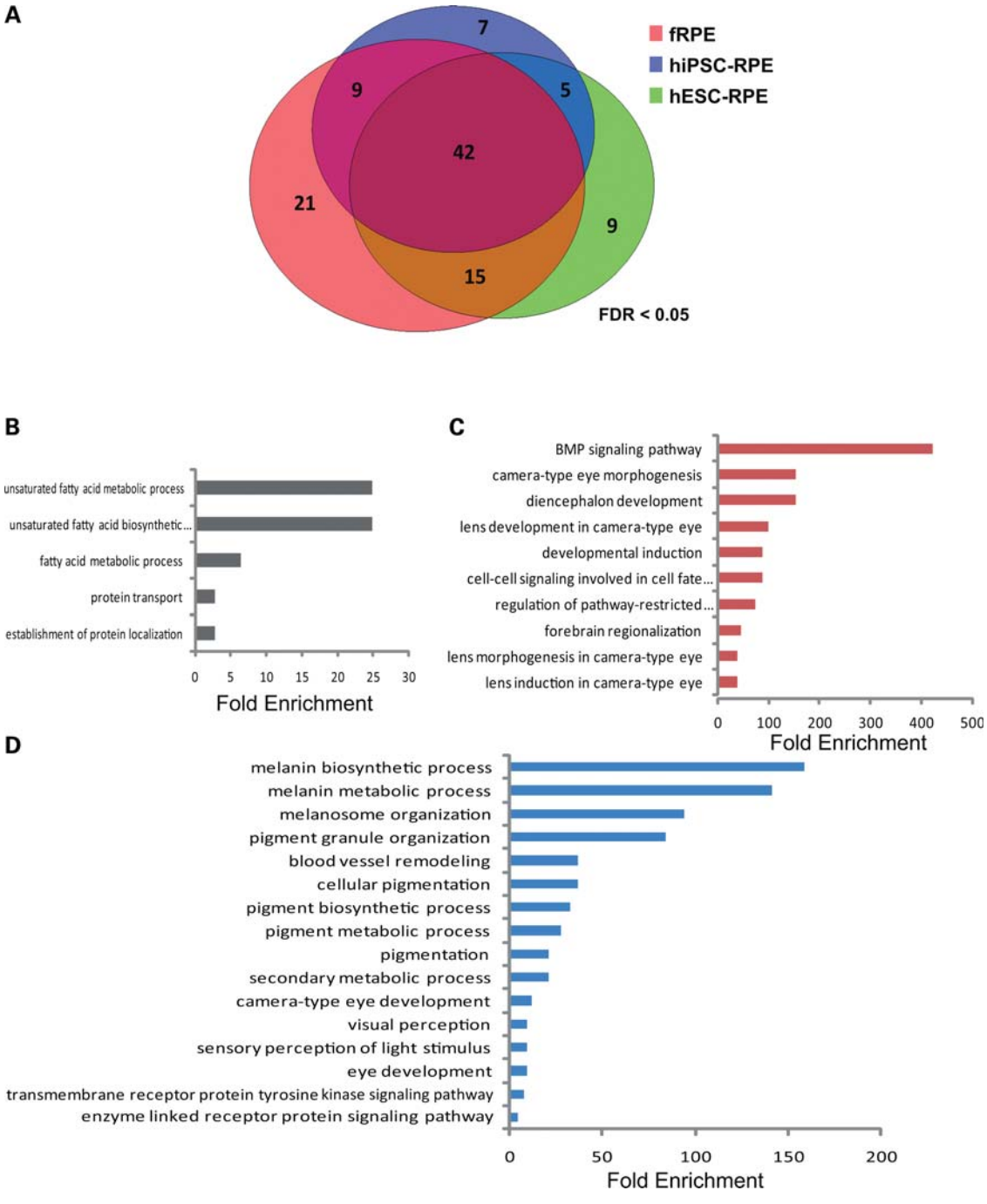

Figure 6. Analysis of RPE signature genes in fRPE, hESC-RPE and hiPSC-RPE. (**A**) The Venn diagram shows the shared/unique genes among 108 selected RPE signature genes for fRPE, hESC-RPE and hiPSC-RPE. (**B**) Functional annotation from gene ontology analysis of 43 fRPE signature genes that are shared with undifferentiated hESCs. (**C**) Twenty-one fRPE genes that are under-expressed in stem-cell-derived RPE cells. (**D**) Forty-two core RPE signature genes that are shared by fRPE and stem-cell-derived RPE cells.

with their role in RPE differentiation pathways (Fig. 6D). These results suggest that despite morphology and functional similarities, genetic profiles of stem-cell-derived RPE cells are moderately different from normal fRPE cells.

Notably, by cross-comparison of the 87 RPE signature genes in fRPE with gene expression in hESC-RPE and hiPSC-RPE cells, we found that 21 signature genes that are exclusive to fRPE, but not shared with stem-cell-derived RPE cells (Fig. 6A, Supplementary Material, Table S5). Gene ontology analysis showed that these genes are involved in various eye development pathways such as BMP signaling, lens development and eye and lens morphogenesis (Fig. 6C). This suggests that stem-cell-derived RPE may lack robust expression of some critical genes that are involved in eye development.

DISCUSSION

The RPE is critical for retinal viability and function and has been the focus for AMD and its therapeutic interventions. Although a significant amount of research has focussed on deriving functional RPE cells from various stem cell sources, little is known about the global transcriptional profiles of these stem-cell-derived RPE cells. In this study, we have derived functional RPE cells from various lines of hESCs and hiPSCs and generated global expression profiles of stem-cell-derived RPE and human fRPE cells. We found that hESC-RPE resembles fRPE more closely than hiPSC-RPE. The expression profiles of hiPSC-RPE suggest that they are in a relatively immature differentiation state. Also, we identified a set of genes that are exclusively expressed in human fRPE. This set of genes may serve as reliable molecular signatures of fRPE and provide future standards for scoring the differentiation state of stem-cell-derived RPE cells. Together, these results offer critical insights into the therapeutic use of stem-cell-derived RPE cells in treating AMD.

Stem-cell-derived RPE cells have a highly similar morphology to human fRPE. These cells arise spontaneously from stem cell sources 3–4 weeks after differentiation, consistent with the differentiation timeline shown by other groups. We observed varying differentiation propensities between cell lines. This may be a result of genetic background differences between each cell line, especially in hiPSCs. Previous reports have shown some cell types are more efficiently reprogrammed (7,21,22); it is possible that these biases are persistent during differentiation to RPE cells.

HESC-RPE and hiPSC-RPE express a panel of RPE gene transcripts similar to cultured fRPE cells. Co-expression of the early RPE development marker, PAX6, with various mature markers suggests that hESC-RPE has some heterogeneity, which may be due to immature cells around the leading edges of hESC-RPE expanding sheets. HESC-RPE were previously shown to expand through a de-differentiation mechanism, which involves pigmented cells showing de-pigmentation, then entering into the active cell cycle before gaining pigmentation again (12). Interestingly, a majority of the RPE-associated markers was detected in hiPSC-RPE, but not the early marker, PAX6, and the late marker, LRAT, suggesting that hiPSC-RPE may be in a unique differentiation state. Recent reports have shown some loci are more resistant to reprogramming in hiPSCs, which may affect the expression of certain genes (9,23,24). There appear to be several discrepancies between hESC-RPE, hiPSC-RPE and primary RPE cells, but it remains unclear whether these differences will affect the utility of stem-cell-derived RPE in the clinical setting.

Global gene expression analysis demonstrated that hESC-RPE resembles fRPE more closely than hiPSC-RPE. Pair-wise comparisons between hESC-RPE to fRPE and hiPSC-RPE to fRPE revealed that stem-cell-derived RPE cells show under-expression of genes involved in visual perception. Interestingly, some of the up-regulated transcripts in hiPSC-RPE are involved in immune responses. This observation is consistent with transcriptional and methylation profile comparisons between hESCs and hiPSCs (unpublished data), suggesting hiPSC-RPE may retain specific reprogramming gene signatures.

Furthermore, we found similar gene expression levels of complement associated proteins previously reported to be associated with AMD in stem-cell-derived RPE and fRPE cells. Allele variants for different complement cascade-associated proteins have been implicated as major risk factors for the predisposition of AMD (25,26). Further analysis of SNPs in each stem cell line is required to determine whether they carry AMD risk variants. Our analysis of aging retina-associated genes shows that cultured stem-cell RPE mimic fRPE and do not show signs of aging. This addresses the concern that extended culture may induce the expression of age-related genes and suggests that culture-derived RPE may be suitable replacements for fRPEs in cell transplantation therapy.

Recent microarray-based studies have identified RPE-specific genes by comparing human RPE with various retinal and somatic tissues (20,27). However, comparisons between two separate studies showed very few RPE signature genes actually overlapped. These discrepancies may arise from differences in the experimental design and tissues used in their respective analyses. We chose to cross-reference our data with Miller's data set due to the more comprehensive nature of their study (20). Using their identified signature gene list, we compared their expression with hESCs and refined the list by excluding genes that are not significantly differentially expressed with hESCs. Surprisingly, a small group of eye developmental genes are uniquely expressed in fRPE but not in stem-cell-derived RPE cells, indicating that several eye development pathways remain underdeveloped in stem-cell-derived RPE cells. It is possible that using different differentiation protocols may yield activation of these pathways in stem-cell-derived RPE cells. Previous studies using directed differentiation to recapitulate *in vivo* development of RPE first directed differentiation toward the neuronal lineage, followed by differentiation toward the RPE fate. It will be important to examine the differences between spontaneous differentiation and directed differentiation and find optimal culture conditions for deriving RPE cells that best resemble native RPE.

Our results highlight significant differences between expression profiles of stem-cell-derived RPE cells and fRPE. To fully realize the potential of stem-cell-derived RPE in cell-based therapy, future work using *in vivo* models will elucidate the utility of stem-cell-derived RPE in restoring vision. This study establishes a standard for expanded analyses of expression profiles in additional cell lines. Our findings represent an important step toward optimizing the future application of stem-cell-derived RPE for transplantation into AMD patients.

MATERIALS AND METHODS

Pluripotent stem cell culture

The hESC lines H9 and HSF1 were maintained as described previously (28). The induced pluripotent stem cell lines HiPS2, HiPS18 and NPC2-iPS#3 were maintained under similar conditions with a 1:1 ratio of hESC medium to conditioned medium. Conditioned medium was prepared by the incubation of hESC medium overnight with MEF cells.

Differentiation, enrichment and culture of pigmented cells

Differentiation of hESCs and hiPSCs to RPE cells followed a previously described protocol with minor modifications (12). All cells were cultured in 10 cm cell culture dish (Corning) or six-well cell culture plates (Costar). HESC-RPE and hiPSC-RPE were formed when hESCs colonies were allowed to become over-confluent on an MEF density of 1×10^4 cm^{-2}. When the borders of individual hESC colonies contacted each other at approximately 7–10 days post-passage, the medium was changed daily using basic hESCs medium lacking bFGF. Pigmented foci appeared in over-confluent hESCs cultures 3–4 weeks after the use of bFGF-deficient hESC medium.

Following formation, pigmented clusters were excised manually using syringe needles under a dissecting microscope. This approach was only possible after a cluster had reached at least 1 mm in diameter. During this procedure, we avoided the surrounding, non-pigmented material prior to placement of the pigmented cluster in 24-well culture dishes coated with growth factor reduced Matrigel^{TM} (BD Biosciences, diluted 1:30). Alternatively, Millicell-HA (Millipore) culture wells were coated with Matrigel. Two to three pigmented foci were placed in each well; hESC-RPE and hiPSC-RPE were allowed to expand on Matrigel for a further 2 months in basic bFGF deficient hESCs medium (media changes every 2–3 days). This time frame was sufficient to yield monolayer sheets of pigmented cells that could be studied further.

Fetal human RPE cell culture

The culture method for fetal human RPE cells has been described previously (16,29). Briefly, fetal human RPE cells from (16–21 weeks gestation) was collected and grown in low calcium Chee's essential modified medium until they proliferated to confluence and released cells into the medium. These non-attached cells were collected and grown for 4–8 months on permeable Millicell-HA culture wells. The culture medium was changed to a 1:1 mixture of normal calcium CEM and Eagle's minimum essential medium, with bovine retinal extract and 1% heat-inactivated calf serum.

Reverse transcription–polymerase chain reaction

Gene expression of stem-cell-derived RPE cells was analyzed by RT–PCR. The experimental procedure is similar to that described previously (28). Primer pairs were adopted from the published literature (12,13).

Immunocytochemistry

Immunocytochemistry was carried out as described (30). Primary antibodies used in the experiment were anti-RPE65 (Chemicon) and ZO1 (Zymed).

Western blotting

Western blotting was carried out on protein samples from cell culture dish containing pigmented sheets of putative RPE cells similar to previously described procedure (30). The primary antibody used in the experiment was RPE65 (1:5000, Chemicon) and GAPDH (1:10 000, Abcam).

ROS phagocytosis assay

The phagocytosis and digestion of mouse rod outer segments (ROSs) by hESC-derived RPE and human fRPE cells, grown on filters in Millicell-HA wells, were assayed as described (31). The cultured cells were incubated with 2×10^6 ROSs per well for 30 min, and then washed with cold Dulbecco's PBS to remove unbound ROSs. Some filters were incubated for a further 2 h. ROSs were labeled with the polyclonal 01 opsin antibody before and after permeabilization of the cells, in order to quantify bound and ingested ROSs. Labeling before permeabilization was followed by a secondary antibody conjugated to Alexa Fluor 488 and after permeabilization by a secondary antibody conjugated to Alexa Fluor 594 (ingested ROSs are therefore labeled only by the second antibody. ROSs that were >1 μm in diameter were counted in each field of view. At least three fields of view were imaged per filter, and each treatment was performed in triplicate.

Microarray

Gene expression was analyzed by RT–PCR of total RNA extracted with TRIzol reagent from cell culture dishes containing pigmented sheets of putative RPE cells. RNA was purified using RNeasy Kit (Qiagen) following the manufacturer's instruction. Sample labeling and microarray processing was performed as detailed in the 'One-Color Microarray-Based Gene Expression Analysis' protocol. The labeling reactions were performed using the Agilent Low RNA Input Linear Amplification Kit in the presence of cyanine 3-CTP (PerkinElmer Life and Analytical Sciences). Fluorescent labeled probes were purified using the Qiagen RNeasy Mini kit (Qiagen) as described by the manufacturer. Dye incorporation was confirmed using nanodrop ND1000. For microarray hybridization, 1000 ng of cyanine 3-labeled cRNA was fragmented and hybridized on Agilent 44K Whole Human genome arrays (G4112A; Agilent Technologies) and incubated at 65°C for 17 h using the Agilent Gene Expression Hybridization Kit. The hybridized microarrays were dissembled at room temperature in Gene Expression Wash Buffer 1, then washed in Gene Expression Wash Buffer 1 at room temperature for 1 min. This was followed by a wash for 1 min in Gene Expression Wash Buffer 2 at an elevated temperature (33°C). The processed microarrays were scanned with the Agilent DNA microarray scanner immediately after washing to prevent ozone degradation and data were extracted with Agilent Feature Extraction software. Microarray data are deposited to GEO database with accession number available upon publication.

Gene expression analysis

Data analysis was carried out using both R and Matlab. R was used for importing, quantile-normalizing and log-transforming Cy3 signal intensity only. Pertinent raw data sets available from the GEO database were similarly normalized and log-transformed. To correct for batch effects, and non-biological variations between different data sets, we implemented batch

effect correction using the ComBat package in R. Hierarchical clustering was performed using Matlab's dendrogram function. PCA analysis was performed using the princomp function and visualized using the mapcaplot graphical interface. Biplots for various pair-wise comparisons were also carried out in Matlab using the scatter plotting function. Differential expression analysis between RPE and ES cells was determined using a combination of *t*-statistic, false discovery rate, and fold change.

SUPPLEMENTARY MATERIAL

Supplementary Material is available at *HMG* online.

Conflict of Interest statement. None declared.

FUNDING

This work is supported by Translational I Grant TR1-272 from California Institute for Regenerative Medicine to X.-J.Y., G.H.T., D.S.W., D.B. and G.F. G.F. is a Carol Moss Spivak Scholar in Neuroscience.

REFERENCES

1. Vugler, A., Lawrence, J., Walsh, J., Carr, A., Gias, C., Semo, M., Ahmado, A., da Cruz, L., Andrews, P. and Coffey, P. (2007) Embryonic stem cells and retinal repair. *Mech. Dev.*, **124**, 807–829.
2. Idelson, M., Alper, R., Obolensky, A., Ben-Shushan, E., Hemo, I., Yachimovich-Cohen, N., Khaner, H., Smith, Y., Wiser, O., Gropp, M. *et al.* (2009) Directed differentiation of human embryonic stem cells into functional retinal pigment epithelium cells. *Cell Stem Cell*, **5**, 396–408.
3. Strauss, O. (2005) The retinal pigment epithelium in visual function. *Physiol. Rev.*, **85**, 845–881.
4. Gehrs, K.M., Anderson, D.H., Johnson, L.V. and Hageman, G.S. (2006) Age-related macular degeneration—emerging pathogenetic and therapeutic concepts. *Ann. Med.*, **38**, 450–471.
5. da Cruz, L., Chen, F.K., Ahmado, A., Greenwood, J. and Coffey, P. (2007) RPE transplantation and its role in retinal disease. *Prog. Retin. Eye Res.*, **26**, 598–635.
6. Haruta, M. (2005) Embryonic stem cells: potential source for ocular repair. *Semin. Ophthalmol.*, **20**, 17–23.
7. Takahashi, K., Tanabe, K., Ohnuki, M., Narita, M., Ichisaka, T., Tomoda, K. and Yamanaka, S. (2007) Induction of pluripotent stem cells from adult human fibroblasts by defined factors. *Cell*, **131**, 861–872.
8. Nishikawa, S., Goldstein, R.A. and Nierras, C.R. (2008) The promise of human induced pluripotent stem cells for research and therapy. *Nat. Rev. Mol. Cell Biol.*, **9**, 725–729.
9. Hochedlinger, K. and Plath, K. (2009) Epigenetic reprogramming and induced pluripotency. *Development*, **136**, 509–523.
10. Yu, J., Vodyanik, M.A., Smuga-Otto, K., Antosiewicz-Bourget, J., Frane, J.L., Tian, S., Nie, J., Jonsdottir, G.A., Ruotti, V., Stewart, R. *et al.* (2007) Induced pluripotent stem cell lines derived from human somatic cells. *Science*, **318**, 1917–1920.
11. Kim, P.G. and Daley, G.Q. (2009) Application of induced pluripotent stem cells to hematologic disease. *Cytotherapy*, **11**, 980–989.
12. Vugler, A., Carr, A.J., Lawrence, J., Chen, L.L., Burrell, K., Wright, A., Lundh, P., Semo, M., Ahmado, A., Gias, C. *et al.* (2008) Elucidating the phenomenon of HESC-derived RPE: anatomy of cell genesis, expansion and retinal transplantation. *Exp. Neurol.*, **214**, 347–361.
13. Buchholz, D.E., Hikita, S.T., Rowland, T.J., Friedrich, A.M., Hinman, C.R., Johnson, L.V. and Clegg, D.O. (2009) Derivation of functional retinal pigmented epithelium from induced pluripotent stem cells. *Stem Cells*, **27**, 2427–2434.
14. Lund, R.D., Wang, S., Klimanskaya, I., Holmes, T., Ramos-Kelsey, R., Lu, B., Girman, S., Bischoff, N., Sauve, Y. and Lanza, R. (2006) Human embryonic stem cell-derived cells rescue visual function in dystrophic RCS rats. *Cloning Stem Cells*, **8**, 189–199.
15. Coffey, P.J., Girman, S., Wang, S.M., Hetherington, L., Keegan, D.J., Adamson, P., Greenwood, J. and Lund, R.D. (2002) Long-term preservation of cortically dependent visual function in RCS rats by transplantation. *Nat. Neurosci.*, **5**, 53–56.
16. Hu, J. and Bok, D. (2001) A cell culture medium that supports the differentiation of human retinal pigment epithelium into functionally polarized monolayers. *Mol. Vis.*, **7**, 14–19.
17. Bergeron-Sawitzke, J., Gold, B., Olsh, A., Schlotterbeck, S., Lemon, K., Visvanathan, K., Allikmets, R. and Dean, M. (2009) Multilocus analysis of age-related macular degeneration. *Eur. J. Hum. Genet.*, **17**, 1190–1199.
18. Yoshida, S., Yashar, B.M., Hiriyanna, S. and Swaroop, A. (2002) Microarray analysis of gene expression in the aging human retina. *Invest. Ophthalmol. Vis. Sci.*, **43**, 2554–2560.
19. Anderson, D.H., Radeke, M.J., Gallo, N.B., Chapin, E.A., Johnson, P.T., Curletti, C.R., Hancox, L.S., Hu, J., Ebright, J.N., Malek, G. *et al.* (2010) The pivotal role of the complement system in aging and age-related macular degeneration: hypothesis re-visited. *Prog. Retin. Eye Res.*, **29**, 95–112.
20. Strunnikova, N.V., Maminishkis, A., Barb, J.J., Wang, F., Zhi, C., Sergeev, Y., Chen, W., Edwards, A.O., Stambolian, D., Abecasis, G. *et al.* (2010) Transcriptome analysis and molecular signature of human retinal pigment epithelium. *Hum. Mol. Genet.*, **29**, 2468–2486.
21. Taura, D., Noguchi, M., Sone, M., Hosoda, K., Mori, E., Okada, Y., Takahashi, K., Homma, K., Oyamada, N., Inuzuka, M. *et al.* (2009) Adipogenic differentiation of human induced pluripotent stem cells: comparison with that of human embryonic stem cells. *FEBS Lett.*, **583**, 1029–1033.
22. Aasen, T., Raya, A., Barrero, M.J., Garreta, E., Consiglio, A., Gonzalez, F., Vassena, R., Bilic, J., Pekarik, V., Tiscornia, G. *et al.* (2008) Efficient and rapid generation of induced pluripotent stem cells from human keratinocytes. *Nat. Biotechnol.*, **26**, 1276–1284.
23. Urbach, A., Bar-Nur, O., Daley, G.Q. and Benvenisty, N. (2010) Differential modeling of fragile X syndrome by human embryonic stem cells and induced pluripotent stem cells. *Cell Stem Cell*, **6**, 407–411.
24. Stadtfeld, M., Apostolou, E., Akutsu, H., Fukuda, A., Follett, P., Natesan, S., Kono, T., Shioda, T. and Hochedlinger, K. (2010) Aberrant silencing of imprinted genes on chromosome 12qF1 in mouse induced pluripotent stem cells. *Nature*, **465**, 175–181.
25. Gold, B., Merriam, J.E., Zernant, J., Hancox, L.S., Taiber, A.J., Gehrs, K., Cramer, K., Neel, J., Bergeron, J., Barile, G.R. *et al.* (2006) Variation in factor B (BF) and complement component 2 (C2) genes is associated with age-related macular degeneration. *Nat. Genet.*, **38**, 458–462.
26. Yates, J.R., Sepp, T., Matharu, B.K., Khan, J.C., Thurlby, D.A., Shahid, H., Clayton, D.G., Hayward, C., Morgan, J., Wright, A.F. *et al.* (2007) Complement C3 variant and the risk of age-related macular degeneration. *N. Engl. J. Med.*, **357**, 553–561.
27. Booij, J.C., ten Brink, J.B., Swagemakers, S.M., Verkerk, A.J., Essing, A.H., van der Spek, P.J. and Bergen, A.A. (2010) A new strategy to identify and annotate human RPE-specific gene expression. *PLoS ONE*, **5**, e9341.
28. Shen, Y., Chow, J., Wang, Z. and Fan, G. (2006) Abnormal CpG island methylation occurs during in vitro differentiation of human embryonic stem cells. *Hum. Mol. Genet.*, **15**, 2623–2635.
29. Hu, J.G., Gallemore, R.P., Bok, D., Lee, A.Y. and Frambach, D.A. (1994) Localization of NaK ATPase on cultured human retinal pigment epithelium. *Invest. Ophthalmol. Vis. Sci.*, **35**, 3582–3588.
30. Feng, J., Chang, H., Li, E. and Fan, G. (2005) Dynamic expression of de novo DNA methyltransferases Dnmt3a and Dnmt3b in the central nervous system. *J. Neurosci. Res.*, **79**, 734–746.
31. Gibbs, D., Kitamoto, J. and Williams, D.S. (2003) Abnormal phagocytosis by retinal pigmented epithelium that lacks myosin VIIa, the Usher syndrome 1B protein. *Proc. Natl Acad. Sci. USA*, **100**, 6481–6486.